Gravitational Wave Astronomy

Riccardo Sturani

Instituto de Física Teórica UNESP

riccardo.sturani@unesp.br

April 9th, 2024 – High-energy astrophysics in the multi-messenger era

A guide to GW observations

Outline

LIGO and Virgo (+KAGRA): very precise rulers

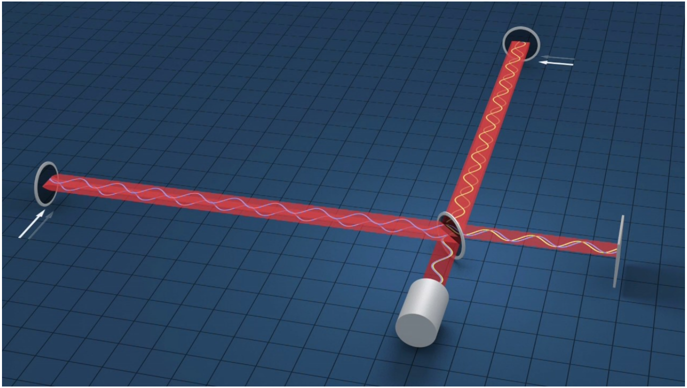

Robert Hurt (Caltech)

Light intensity $\propto$ light travel difference in perpendicular arms
Effective optical path increased by factor $N \sim 500$ via Fabry-Perot cavities
Phase shift $\Delta\phi \sim 10^{-8}$ can be measured $\sim 2\pi N \Delta L/\lambda \rightarrow \Delta L \sim 10^{-15}/N$ m

Noise budget

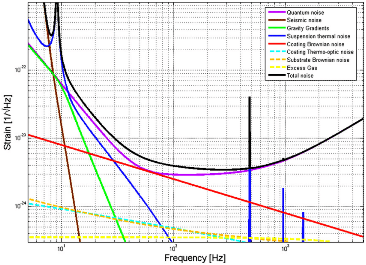

Barriga et al., CQG (2013) 084005

Why $Hz^{-1/2}$? Detector's FoM is *noise spectral density* $S_n(f)$:

$$\langle \tilde{n}(f)\tilde{n}(f')\rangle = S_n(f)\delta(f-f')$$

i.e. $S_n(f_i) \sim |\tilde{n}(f_i)|^2 \Delta f$. Best sensitivity for an interferometer for $\frac{\lambda_{GW}}{2} \gtrsim L \implies$ $f_{GW\ best} \lesssim \frac{c}{4\pi L} \sim 160\mathrm{Hz}\left(\frac{L}{150\mathrm{km}}\right)^{-1}$

Almost omnidirectional detectors

Detectors measure h_{det}: linear combination $F_+ h_+ + F_\times h_\times$

L H

-1 0 1

F_+

$F_\times$

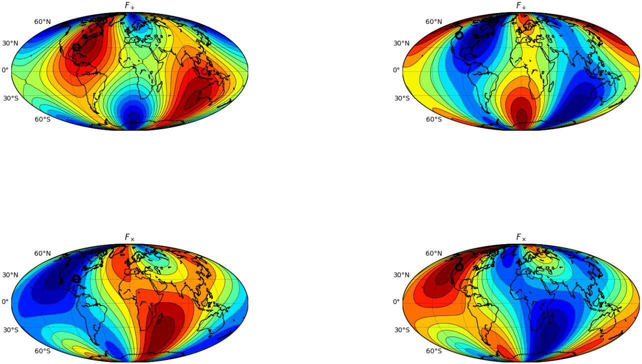

$h_{+,\times}$ depend on source

pattern functions $F_{+,\times}$ depend on orientation source/detector

Almost omnidirectional detectors

Detectors measure h_{det}: linear combination $F_+ h_+ + F_\times h_\times$

L V

-1 0 1

F_+

$F_\times$

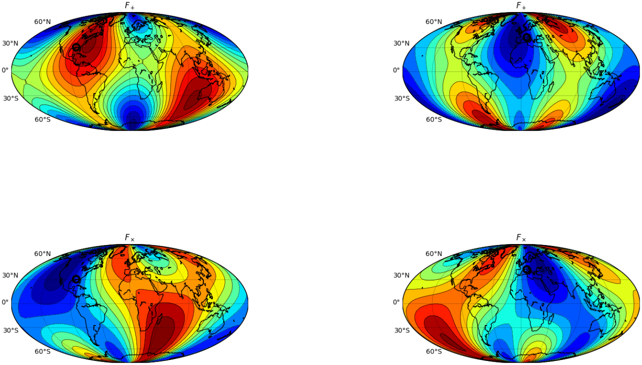

$h_{+,\times}$ depend on source

pattern functions $F_{+,\times}$ depend on orientation source/detector

Pattern functions: $\sqrt{F_+^2 + F_\times^2}$

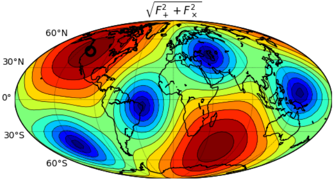

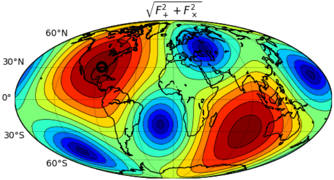

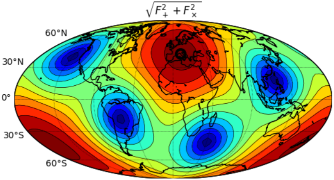

The LIGO and Virgo observatories

- Observation run **O1** Sept '15 - Jan '16 $\sim$ 130 days, with 49.6 days of actual data, PRX (2016) 4, 041014, 2 detectors, 3BBH
- **O2** Dec. '16 – Jul'17 2 det's + Aug '17 3 det's 3(+4) BBH + 1BNS in double (triple) coinc.
- **O3a**: 3 detectors, Apr - Sep 2019, 39 detections
- **O3b**: Nov 1st – Mar 27th 2020 $\rightarrow$ 90 detections
- **O4a**: Ongoing (since May 24th) $\rightarrow$ end 2024

KAGRA

Additional *underground*, *cryogenic* detector

KAGRA Collaboration, Galaxies 10 (2022) 3, 63

Outline

Stellar ($< 100 M_\odot$) compact object with known masses

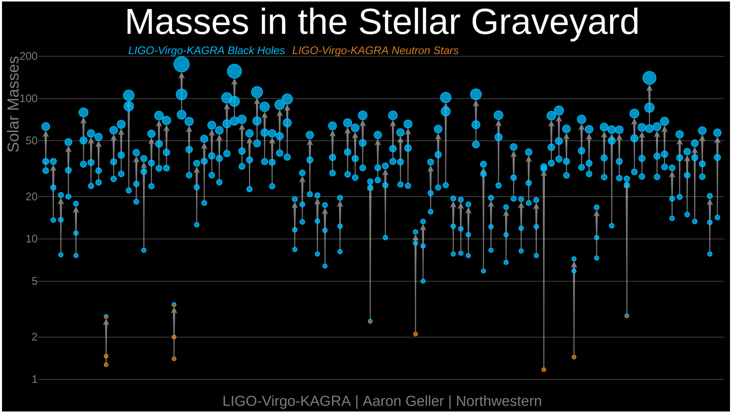

Frequency 10-10^3 Hz determines size of sources

Remnant of various GW events represent first Intermediate Mass Black Holes ($> 10^2 M_\odot$) – SuperMassive BHs $\gtrsim 10^5 M_\odot$ (up to $10^9 M_\odot$)

Sky localization: sample events

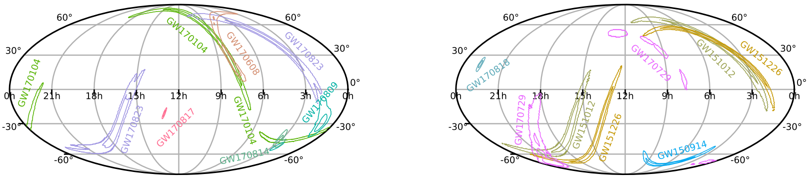

One needs 3 detectors to triangulate the source (useful info from pattern functions)

Distances between 40 Mpc and $\sim$ 5 Gpc ($\pm$20%)

(Milky Way's size $\sim 30\mathrm{kpc}$, Galaxy-Galaxy $\sim$ 4Mpc)

Image by Leo Singer, http://www.ligo.org

Little is known so far about spins

$$\vec{S}_i = m_i^2 \chi_i,\ \chi_{eff} \equiv \frac{m_1 \vec{\chi}_1 \cdot \vec{L} + m_2 \vec{\chi}_2 \cdot \vec{L}}{M},\ M = m_1 + m_2$$

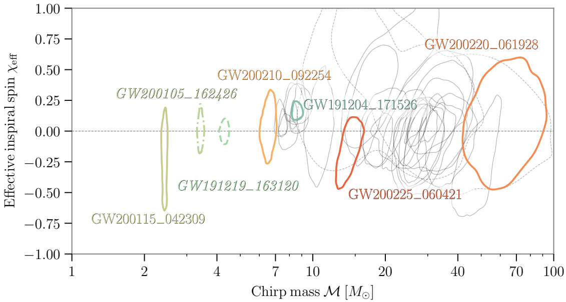

More unequal-masses systems bear larger spin imprint: $|\vec{L}| \sim \frac{m_1 m_2}{v}$

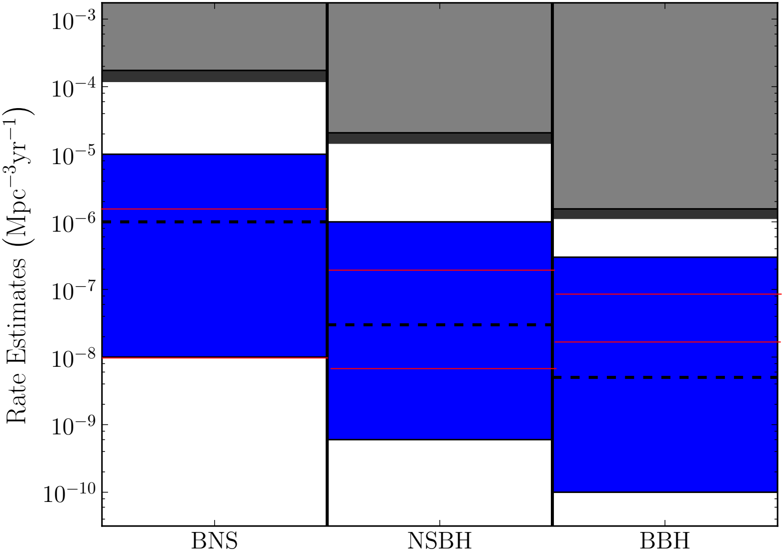

Astro predictions, measures from O1/O2/O3. Galaxy density $\sim 2 \times 10^{-2} Mpc^{-3}$

LIGO/Virgo CQG ('10) 27 173001, PRX ('16), APJ (2016), PRL 119 ('17)

LIGO/Virgo/KAGRA's prospects

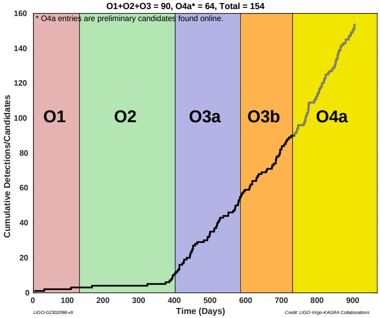

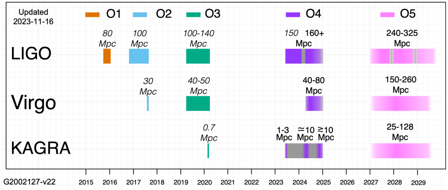

https://dcc.ligo.org/LIGO-G2302098

Future with ET and LISA looks very loud

Future 3rd generetaion detectors (Einstein Telescope, Cosmic Explorer)/space telescope LISA will detect CBC signals with SNR $10 - 10^2$, with few golden events with SNR $\sim 10^3$.

Templates few % accurate OK for characterising a source with SNR $O(10)$ (typical for LIGO/Virgo)

for SNR $\sim 10^3$ residual after extracting that source will have SNR $\sim O(10)$

1. baising parameter estimation
2. contaminating the extraction of additional sources.

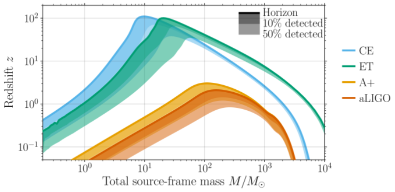

Hall, Evans CQG (2019), 1902.09485

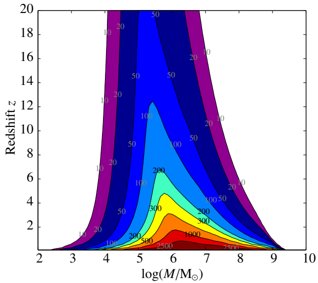

Amaro-Seoane+, GW Notes 6 (2013),

Nanograv (& PTA)

Monitoring irregularities in pulsar signals one can infer GW strength:

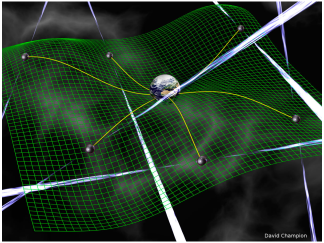

Credit: David Champion

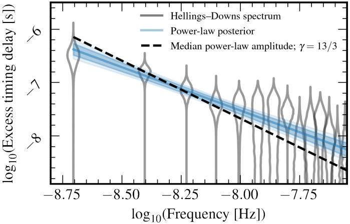

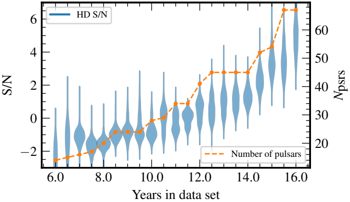

$$T = 16.03\text{yr} = \frac{1}{2\text{nHz}},\ f_i = i/T$$

Nanograv, APJ Lett. (2023) 2306.16213

Sensitivities and duration

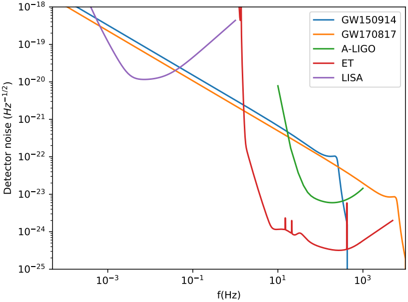

$\tilde{h}(f) \sim \frac{f^{-7/6}(GM_c)^{5/6}}{D_L} e^{i\psi(f)}$

Signal duration controlled by $\frac{5}{256\pi}(\pi M_c f_i)^{-5/3} = 30 \times \frac{1}{\eta}\left(\frac{M}{20M_\odot}\right)^{-5/3}\left(\frac{f_i}{20\mathrm{Hz}}\right)^{-5/3}$

$\Delta t_{i\to f} \sim \frac{5}{256\pi}(\pi G M_c)^{-5/3}\left(f_i^{-8/3} - f_m^{-8/3}\right) \to$

$$\frac{5}{256\pi}(\pi M_c f_i)^{-5/3} \times \begin{cases} \frac{1}{f_i} & \Delta t < t_{exp} \\ \frac{\Delta f}{f_i^2} & \Delta t > t_{exp} \end{cases}$$

Sensitivities and duration

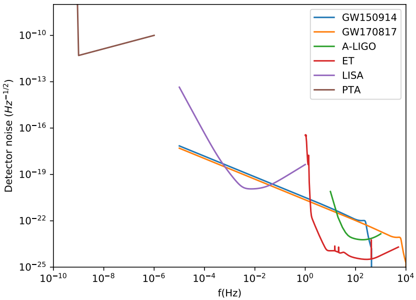

$$\tilde{h}(f) \sim \frac{f^{-7/6}(GM_c)^{5/6}}{D_L} e^{i\psi(f)}$$

Signal duration controlled by $\frac{5}{256\pi}(\pi M_c f_i)^{-5/3} = 30 \times \frac{1}{\eta}\left(\frac{M}{20M\odot}\right)^{-5/3}\left(\frac{f_i}{20\mathrm{Hz}}\right)^{-5/3}$

$$\Delta t_{i\to f} \sim \frac{5}{256\pi}(\pi G M_c)^{-5/3}\left(f_i^{-8/3} - f_m^{-8/3}\right) \to$$

$$\frac{5}{256\pi}(\pi M_c f_i)^{-5/3} \times \begin{cases} \frac{1}{f_i} & \Delta t < t_{exp} \\ \frac{\Delta f}{f_i^2} & \Delta t > t_{exp} \end{cases}$$

Outline

Wave generation: localized sources

Einstein formula relates h_{ij} to the source quadrupole moment Q_{ij}

$$
\begin{aligned}
Q_{ij} &= \int d^3x\rho\left(x_ix_j - \frac{1}{3}\delta_{ij}x^2\right), \qquad v^2 \simeq G_N M/r\,, \quad \eta \equiv m_1 m_2/M^2 \\
h_{ij} &\sim g(\theta_{LN})\frac{2G_N}{D}\frac{d^2Q_{ij}}{dt^2} \simeq \frac{2G_N\eta M v^2}{D}\cos(2\phi(t)) \\
f &= 2\mathrm{kHz}\left(\frac{r}{30\mathrm{Km}}\right)^{-3/2}\left(\frac{M}{3M_\odot}\right)^{1/2} < f_{Max} \simeq 12kHz\left(\frac{M}{3M_\odot}\right)^{-1} \\
v &= 0.3\left(\frac{f}{1\mathrm{kHz}}\right)^{1/3}\left(\frac{M}{M_\odot}\right)^{1/3} < \frac{1}{\sqrt{6}}
\end{aligned}
$$

Geometric factor $g(\theta_{LN})$ takes account of transversality projection (angular momentum L of the binary, observation direction N)

$$
\begin{aligned}
h_+ &\sim \frac{1+\cos^2(\theta_{LN})}{2}\,\eta\frac{Mv^2}{D}\cos\phi(t_s/M,\eta,S_i^2/m_i^4,\ldots) \\
h_\times &\sim \cos(\theta_{LN})\,\eta\frac{Mv^2}{D}\sin\phi(t_s/M,\eta,\ldots)
\end{aligned}
$$

Amplitudes of 2 polarizations modulated by θ_{LN} ($h \nearrow$ for $\theta_{LN} \searrow_0$), never both vanishing unlike dipolar motion for the electromagnetic case Λ breaks scaling Mvs.$1+z$ degeneracy.

Wave generation: localized sources

Einstein formula relates h_{ij} to the source quadrupole moment Q_{ij}

$$
\begin{aligned}
Q_{ij} &= \int d^3x\rho\left(x_ix_j-\frac{1}{3}\delta_{ij}x^2\right)\,, \qquad v^2\simeq G_NM/r\,, \quad \eta\equiv m_1m_2/M^2 \\
h_{ij} &\sim g(\theta_{LN})\frac{2G_N}{D}\frac{d^2Q_{ij}}{dt^2}\simeq\frac{2G_N\eta Mv^2}{D}\cos(2\phi(t)) \\
f &= 2\mathrm{kHz}\left(\frac{r}{30\mathrm{Km}}\right)^{-3/2}\left(\frac{M}{3M_\odot}\right)^{1/2}<f_{Max}\simeq 12kHz\left(\frac{M}{3M_\odot}\right)^{-1} \\
v &= 0.3\left(\frac{f}{1\mathrm{kHz}}\right)^{1/3}\left(\frac{M}{M_\odot}\right)^{1/3}<\frac{1}{\sqrt{6}}
\end{aligned}
$$

Geometric factor $g(\theta_{LN})$ takes account of transversality projection (angular momentum L of the binary, observation direction N)

$$
\begin{aligned}
h_+ &\sim \frac{1+\cos^2(\theta_{LN})}{2}\,\eta\frac{M(1+z)v^2}{D(1+z)}\cos\phi(t_O/(M(1+z)),\eta,S_i^2/m_i^4,\ldots) \\
h_\times &\sim \cos(\theta_{LN})\,\eta\frac{M(1+z)v^2}{D(1+z)}\sin\phi(t_O/(M(1+z)),\eta,\ldots)
\end{aligned}
$$

Amplitudes of 2 polarizations modulated by θ_{LN} ($h\nearrow$ for $\theta_{LN}\searrow_0$), never both vanishing unlike dipolar motion for the electromagnetic case Λ breaks scaling Mvs.$1+z$ degeneracy

Wave generation: localized sources

Einstein formula relates h_{ij} to the source quadrupole moment Q_{ij}

$$
\begin{aligned}
Q_{ij} &= \int d^3x\rho\left(x_i x_j - \frac{1}{3}\delta_{ij}x^2\right), \qquad v^2 \simeq G_N M/r\,, \quad \eta \equiv m_1 m_2/M^2 \\
h_{ij} &\sim g(\theta_{LN})\frac{2G_N}{D}\frac{d^2 Q_{ij}}{dt^2} \simeq \frac{2G_N\eta M v^2}{D}\cos(2\phi(t)) \\
f &= 2\mathrm{kHz}\left(\frac{r}{30\mathrm{Km}}\right)^{-3/2}\left(\frac{M}{3M_\odot}\right)^{1/2} < f_{Max} \simeq 12kHz\left(\frac{M}{3M_\odot}\right)^{-1} \\
v &= 0.3\left(\frac{f}{1\mathrm{kHz}}\right)^{1/3}\left(\frac{M}{M_\odot}\right)^{1/3} < \frac{1}{\sqrt{6}}
\end{aligned}
$$

Geometric factor $g(\theta_{LN})$ takes account of transversality projection (angular momentum L of the binary, observation direction N)

$$
\begin{aligned}
h_+ &\sim \frac{1+\cos^2(\theta_{LN})}{2}\eta\frac{\mathcal{M}v^2}{d_L}\cos\phi(t_O/\mathcal{M},\eta,S_i^2/m_i^4,\ldots) \\
h_\times &\sim \cos(\theta_{LN})\,\eta\frac{\mathcal{M}v^2}{d_L}\sin\phi(t_O/\mathcal{M},\eta,\ldots)
\end{aligned}
$$

Amplitudes of 2 polarizations modulated by θ_{LN} ($h \nearrow$ for $\theta_{LN} \searrow_0$), never both vanishing unlike dipolar motion for the electromagnetic case

h sensitive to red-shifted masses $M \to M(1+z) \equiv \mathcal{M}$

Matched filtering

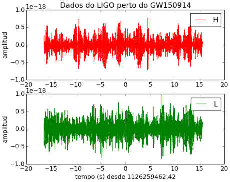

×

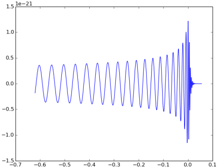

/

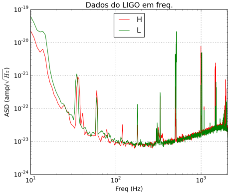

2

Matched filtering

2

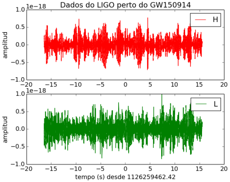

×

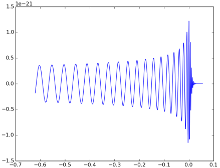

/

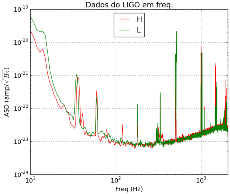

=

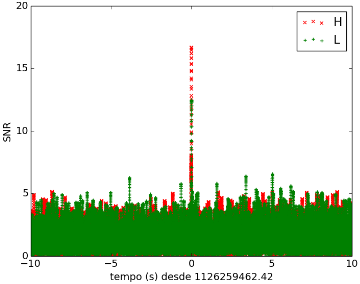

Data from https://losc.ligo.org/events/GW150914/

Outline

The importance of theoretical modeling

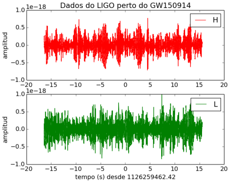

×

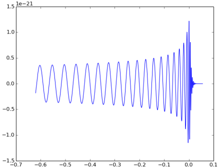

/

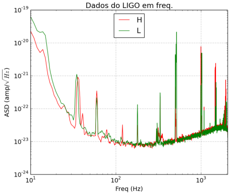

2

The importance of theoretical modeling

2

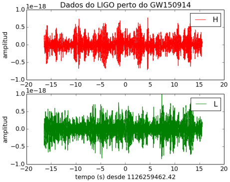

×

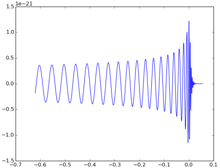

/

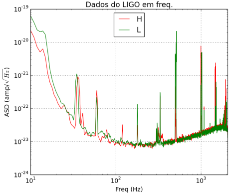

=

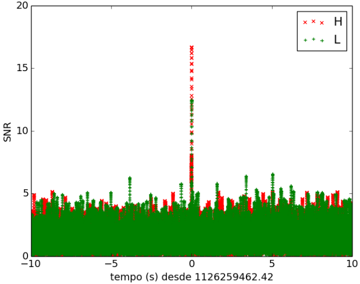

Data from https://losc.ligo.org/events/GW150914/

Fundamental GR: inspiral analytic model

Inspiral $h = A\cos(\phi(t))$ $\qquad \frac{\dot{A}}{A} \ll \dot{\phi}$

Virial relation:

$$v \equiv (G_N M\pi f_{GW})^{1/3} \qquad \eta = \frac{m_1 m_2}{(m_1+m_2)^2}$$

$$\begin{aligned} E(v) &= -\frac{1}{2}\eta M v^2 \left(1 + \#(\eta, S_i/m_i^2)v^2 + \#(\eta, S_i/m_i^2)v^4 + \dots\right) \\ P(v) \equiv -\frac{dE}{dt} &= \frac{32}{5G_N} v^{10} \left(1 + \#(\eta, S_i/m_i^2)v^2 + \#(\eta, S_i/m_i^2)v^3 + \dots\right) \end{aligned}$$

E(v)(P(v)) known up to 3(3.5)PN

$$\begin{aligned} \frac{1}{2\pi}\phi(T) &= \frac{1}{2\pi}\int^T \omega(t)dt = -\int^{v(T)} \frac{\omega(v)dE/dv}{P(v)}dv \\ &\sim \int \left(1 + \#(\eta, S_i/m_i^2)v^2 + \dots + \#(\eta, S_i/m_i^2)v^6 + \dots\right)\frac{dv}{v^6} \end{aligned}$$

Fundamental GR: inspiral analytic model

Inspiral $h = A\cos(\phi(t))$ $\quad \frac{\dot{A}}{A} \ll \dot{\phi}$

Virial relation:

$$v \equiv (G_N M\pi f_{GW})^{1/3} \qquad \eta = \frac{m_1 m_2}{(m_1+m_2)^2}$$

$$E(v) = -\frac{1}{2}\eta M v^2 \left(1 + \#(\eta, S_i/m_i^2)v^2 + \#(\eta, S_i/m_i^2)v^4 + \ldots\right)$$

$$P(v) \equiv -\frac{dE}{dt} = \frac{32}{5G_N} v^{10} \left(1 + \#(\eta, S_i/m_i^2)v^2 + \#(\eta, S_i/m_i^2)v^3 + \ldots\right)$$

E(v)(P(v)) known up to 3(3.5)PN

$$\frac{1}{2\pi}\phi(T) = \frac{1}{2\pi}\int^T \omega(t)dt = -\int^{v(T)} \frac{\omega(v)dE/dv}{P(v)}dv$$

$$\sim \int \left(1 + \#(\eta, S_i/m_i^2)v^2 + \ldots + \#(\eta, S_i/m_i^2)v^6 + \ldots\right)\frac{dv}{v^6}$$

PN Coefficients (absorption $\sim v^8$, tidal $\sim v^{10}$)

Looking for source fingerprints

M_c fixed M fixed

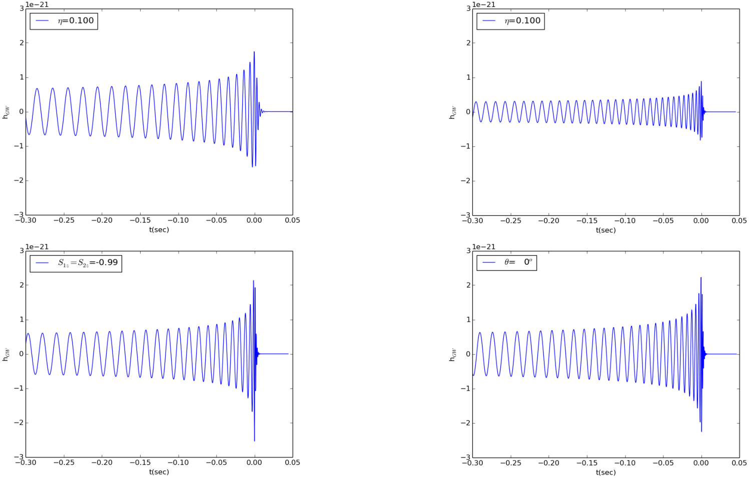

1PM potential

Out of different ways of computing 2-body Post-Minkowskian expansion e.g. 1PM $O(G_N^1)$ potential gravity coupled to particle world-lines:

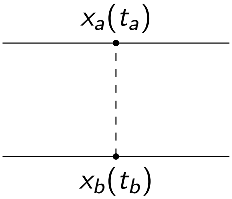

$$V^{(1)}_{PM}(x_a^\mu - x_b^\mu) = G_N T^a_{\mu\nu} T^b_{\rho\sigma} \Delta^{\mu\nu,\rho\sigma} \int \frac{d^4k}{(2\pi)^4} \frac{e^{ik^\mu(x_{a\mu} - x_{b\mu})}}{|\mathbf{k}|^2 - k_0^2 + \epsilon \,\mathrm{terms}}$$

PM complicates

At higher order things rapidly complicate

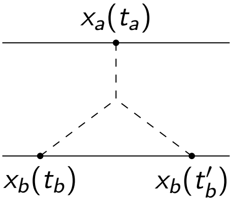

$$\begin{aligned} V^{(2PM)} &\supset G_N^2 m_1 m_2^2 \int d^4p\, e^{ip_\mu(x_a^\mu(t_a)-x_b^\mu(t_b))}\frac{p^\alpha p^\beta}{p^2}\int d^4k\,\frac{e^{ik^\mu(x_b^\mu(t_b)-x_b^\mu(t'_b))}}{(p-k)^2k^2} \\ &= G_N^2 m_1 m_2^2 \int d^4p\, e^{ip_\mu(x_a^\mu(t_a)-x_b^\mu(t_b))}\frac{p^\alpha p^\beta}{p^2}\Delta(p^\mu(x_{2\mu}(t_b)-x_{2\mu}(t'_b))) \end{aligned}$$

These kinds of "conservative" diagrams computed up to 4PM order post-Newtonian approximation trades knowledge over the full trajectory with knowledge of all derivatives of the trajectory at equal time (PN approximation)

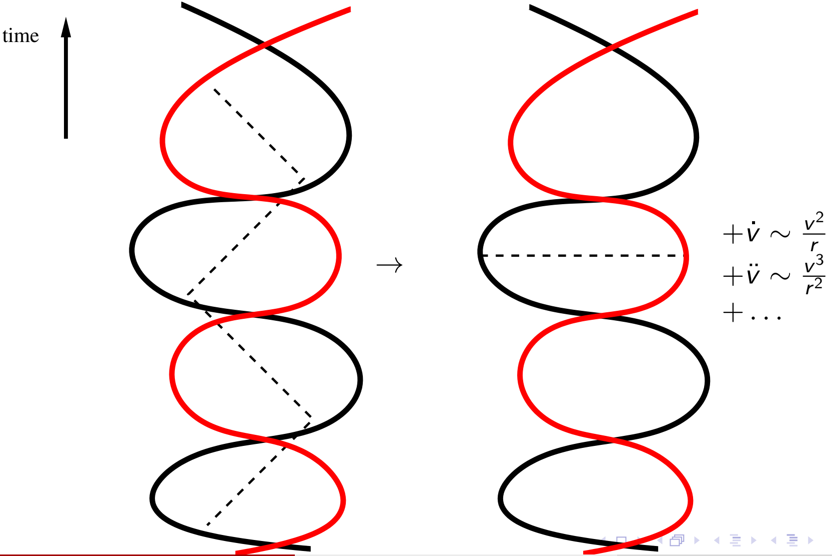

Near zone conservative dynamics

The potential V (via Feynman Green function): 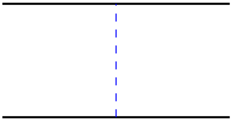

$$
\begin{aligned}
V &\propto \int dk_0 d^3k \frac{e^{-ik_0 t_{12}+i\vec{k}\cdot(\vec{x}_1(t_1)-\vec{x}_2(t_2))}}{k^2-k_0^2-i\epsilon} = \int dk_0 d^3k \frac{e^{-ik_0 t_{12}+i\vec{k}\cdot\vec{x}_{12}}}{k^2}\left(1+\frac{k_0^2}{k^2}+\ldots\right)\\
&= \delta(t_1-t_2)\int d^3k \frac{e^{i\vec{k}\cdot\vec{x}_{12}}}{k^2}\left(1+\frac{\partial_{t_1}\partial_{t_2}}{k^2}+\ldots\right)\\
&= \int d^3k \frac{e^{i\vec{k}\cdot\vec{x}_{12}}}{k^2}\left(1-\frac{\vec{k}\cdot\vec{v}_1\vec{k}\cdot\vec{v}_2}{k^2}+\ldots+\frac{\vec{k}\cdot\frac{d^{n-1}\vec{v}_1}{dt^{n-1}}\vec{k}\cdot\frac{d^{n-1}\vec{v}_2}{dt^{n-1}}}{k^{2n}}\right)
\end{aligned}
$$

"Breaking" the propagator enormous simplificaition, but introduces spurious divergences:
Near zone amplitude integrands clearly bad behaved for $k \to 0$ at high PN-order
Straightforward fix: add the contribution of far-zone, for demonstration see e.g.

Manohar+ '07, Jentzen '12, Blumlein+ '20

EFT and amplitude: tale of a happy marriage

The main obstruction to scalability of the NRGR PN calculation program is the computation of master integrals
E.g. in the static 4PN sector (i.e. G_N^5) one meets

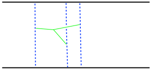

$$= -\mathrm{i}\,(8\pi G_N)^5 \left(\frac{(d-2)}{(d-1)}\; m_1 m_2\right)^3$$

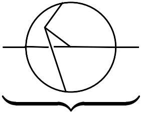

$$\int_{k_{1,2,3,4}} \frac{N_{50}}{k_1^2 \;\; k_2^2 \;\; k_3^2 \;\; k_4^2 \;\; k_{12}^2 \;\; k_{34}^2 \;\; \hat{k}_{24}^2 \;\; p_{13}^2 \;\; \hat{p}_{14}^2}$$

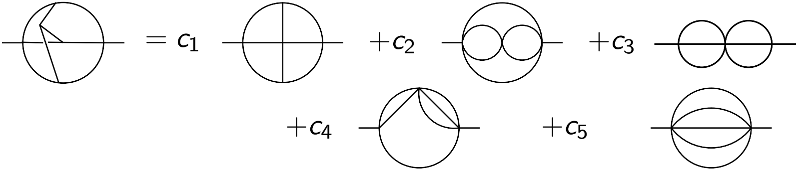

in terms of 4-loop self-energy diagrams in gauge theory

Reduction in terms of master integrals

No new master integrals at 5PN, 4PN ones did it all

Foffa, Mastrolia, RS, Sturm '17

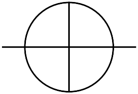

$$= \frac{e^{2\varepsilon\gamma_E}}{s^{2-2\varepsilon}\,(4\pi)^{4+2\varepsilon}}\left\{\frac{1}{2\varepsilon^2}-\frac{1}{2\varepsilon}-4+\frac{\pi^2}{24}\right.$$
$$\left.-\varepsilon\left[9-\pi^2\left(\frac{13}{8}-\log 2\right)-\frac{77}{6}\zeta_3\right]+\mathcal{O}\left(\varepsilon^2\right)\right\}$$

Numerical result obtained via Summertime by Lee& Mingulov
analytic result via PSLQ algorithm, fitting trascendentals to numerical result

Confirmed up to $O(\varepsilon^0)$ by Damour, Jaranowski '18

Summary: 2 body dynamics expansions (spin-less)

Post-Minkowskian expansion parameter is $G_N M/r$, vs PN expansion

$$\mathcal{L} = -Mc^2 + \frac{\mu v^2}{2} + \frac{GM\mu}{r} + \frac{1}{c^2}[\ldots] + \frac{1}{c^4}[\ldots]$$

Terms known so far

		N	1PN	2PN	3PN	4PN	5PN	...
0PM	1	v^2	v^4	v^6	v^8	v^{10}	v^{12}	...
1PM		$1/r$	v^2/r	v^4/r	v^6/r	v^8/r	v^{10}/r	...
2PM			$1/r^2$	v^2/r^2	v^4/r^2	v^6/r^2	v^8/r^2	...
3PM				$1/r^3$	v^2/r^3	v^4/r^3	v^6/r^3	...
4PM					$1/r^4$	v^2/r^4	v^4/r^4	...
5PM						$1/r^5$	v^2/r^5	...
...							$1/r^6$(!)	...

Different approximation methods

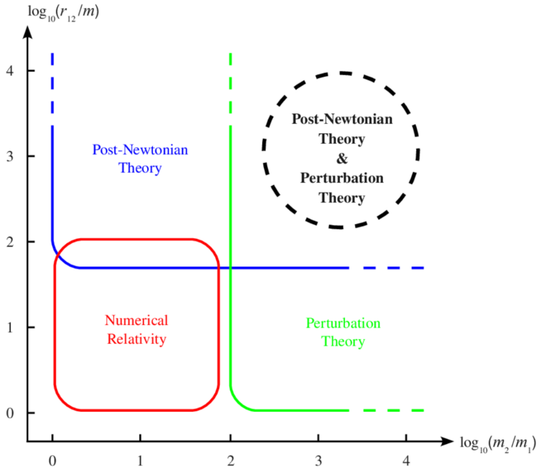

Blanchet et al. arXiv:1007.2614

Bini, Damour, Geralico in PRL ('19)+ completed 4PM dynamics from various input

Numerical relativity solution are expensive for large separation (large orbital scale) and large mass ratios (long dynamical evolution time)

Template bank and extrinsic parameters

Matched filter: $MF(h) \equiv 2\int_0^\infty \frac{\left(\tilde h_d(f)\tilde h_t^*(f)+\tilde h_d(f)^*\tilde h_t(f)\right)}{S_n(f)} fd\log f$, $SNR(h)=\sqrt{MF(h,h)}$

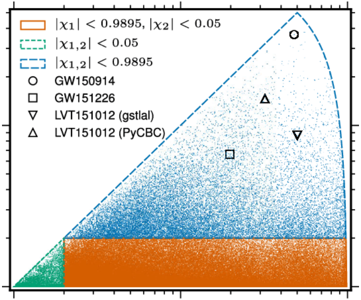

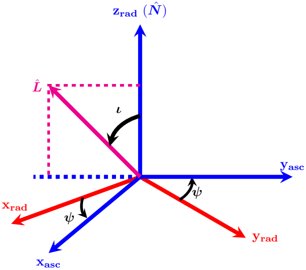

LIGO/Virgo, PRX (2016) 4, 041015, arXiv:1606.04856

J. Mendonça, RS, PRD (2023), arXiv:2302.03676

Parameters: $\underbrace{m_1, m_2, \vec\chi_1, \vec\chi_2}_{intrinsic},\ \underbrace{t, D_L, \overbrace{\theta,\alpha}^{sky\ loc.}, \overbrace{\psi,\iota,\phi}^{Euler\ angles}}_{extrinsic}$

Distance reach

Gravitational Wave Detector Network

Operational Snapshot as of Dec. 7, 2023 02:09:27 UTC

Detector	Status	Duration [hh
GEO600	Unlocked	01:28
LIGO Hanford	Observing	03:04
LIGO Livingston	Observing	02:50
Virgo	Down	>99:00
KAGRA	No data	

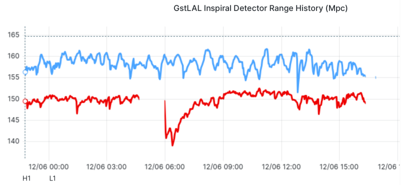

https://online.igwn.org/

How many more?

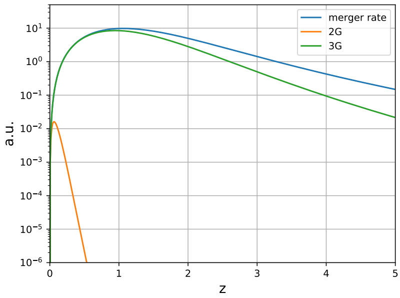

Leandro, Marra, RS PRD '21

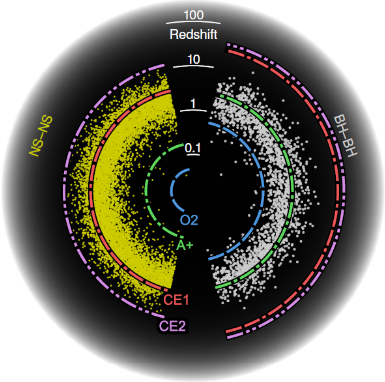

arXiv:1903.04615

What have we learnt?

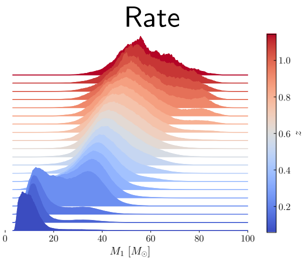

Rinaldi+ 2310.03074

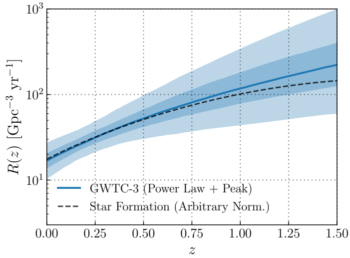

LIGO/Virgo/KAGRA arxiv:2111.03634

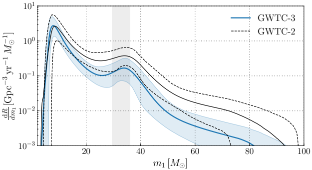

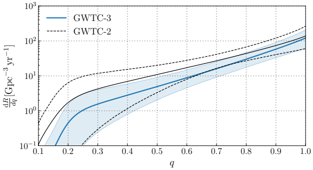

Testing GR

Within the PN parametrization of the GWform phase ($v^3 \equiv \pi G M f$):

$$\tilde{\psi}(f) = \frac{3}{128\eta v^5}\left[\frac{\delta\phi_{-2}}{v^2} + (1+\delta\phi_0) + \delta\phi_1 v + (1+\delta\phi_2)\, v^2 + \dots\right]$$

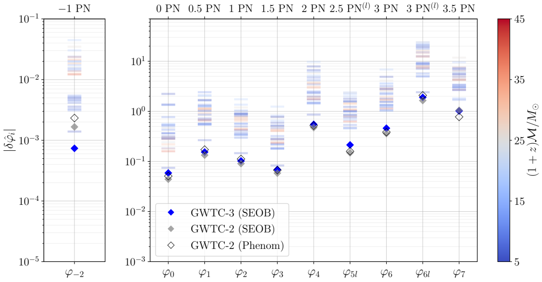

LIGO/Virgo/KAGRA arXiv:2112.06861

Better constraints than binary pulsars (apart from $\delta\phi_0 \lesssim 10^{-5}$, and $\delta\phi_{-2}$)

Nair, Yunes PRD (2020) arXiv:2002.02030

Outline

The importance to know distance and redshift

Luminosity distance vs. redshift: $D_L H_0 = z + O(z^2)$

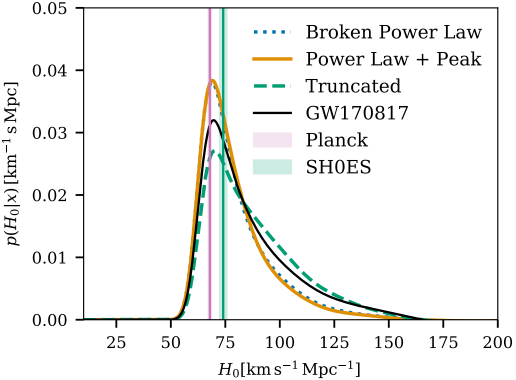

H_0 determination from EM bright 1 standard candle and 46 dark ones, short-circuiting with galaxy survey catalog GLADE+ Dálya et al. arXiv:2110.06184

LIGO/Virgo/KAGRA arXiv:2111.03604

Black sirens

Information also stored in black sirens if *statistical distribution* of merger known (with hyper-parameter τ)

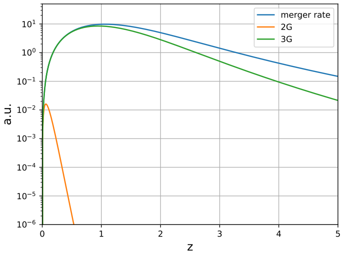

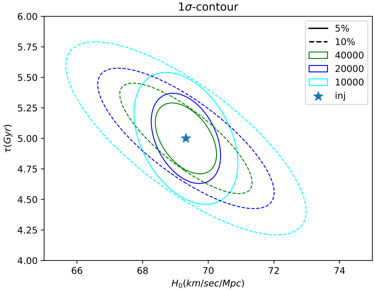

Worst prior knowledge of the redshift distribution (modeling merger rate with more hyper-parameters) degrades predictive power of cosmo pars

Opportunity: fit cosmology and population property

H. Leandro, V. Marra, RS PRD '21

Outline

Summary

- Gravitational Wave Astronomy is a young and fast growing science, its impact will go beyond astronomy
- Field theory methods to solve the 2-body problem in GR are being used as efficient tools for computations from first-principle
- For future developments going to higher order will lead to new master integrals, stumbling block for any perturbative method (PN, PM...)
- Accuracy improvement expected for cosmological parameter/population properties